Quantum Neural Network

- Optical Neural Networks operating at the Quantum Limit -

Preface

We describe the basic concepts, operational principles and expected performance of a novel computing machine, "quantum neural network (QNN)", in this white paper.

There are at least three quantum computing models proposed today: they are unitary quantum computation, adiabatic quantum computation and dissipative quantum computation models. As summarized in Table I, the unitary quantum computation model[1] should be realized in a system well isolated from external worlds (reservoirs) so that the internal quantum states are protected from any decoherence effect. A gate-based quantum computer, consisting of sequential one-bit and two-bit gates, implements this quantum computational model.Only after whole computation processes are completed with unitary rotation of state vectors (qubits), the computational result is extracted by carefully designed quantum interference processes and projective measurements[1, 2]. A theoretical description of this quantum computational model is well established and a physical picture is transparent. However, such a quantum system is not robust against external noise injection and gate errors. This type of quantum computer is a linear interferometer in its very nature and good at finding a hidden period or structure if a given problem has indeed the periodicity[2] or the specific structure[1]. It is shown that the adiabatic quantum computation is mathmatically equivalent to the unitary quantum computation[3] and the above vulnerability to external noise injection is also the case for the adiabatic quantum computation to some extent.

If a given mathematical problem does not have any structure, however, the unitary quantum computation is not necessary efficient in finding a solution. Combinatorial optimization problems, such as traveling salesman problems (TSP), quadratic assignment problems (QAP), satisfiability problems (k-SAT) and maximum cut problems (MAX-CUT), do not have such internal periodicity or specific structures, for which the Grover algorithm is known as an optimum method for the unitary quantum computation to find the solution[4]. In Grover's algorithm, the initial state has equal probability amplitudes for all candidate states of 2^N, i.e. the probability amplitude of each state is $1/\sqrt{2^N}$, where N is the problem size

Table I: Two quantum computational models.

	Unitary quantum computation [1,2]	Dissipative quantum computation [5,6]
Realization	Sequential gates	Neural network
Principle	Unitary rotation of state vectors in a closed system	Self-stabilized ordering in an open system
Proposal	Deutsch (1985) : quantum parallelism Shor (1994) : quantum algorithm	Zurek (2003) : quantum Darwinism and quantum chaos Verstraete, Wolf, and Cirac (2008) : quantum algorithm
Pros	Transparent physics	Robust against noise and error
Cons	Vulnerable to noise and error	Complicated physics
Applications	Problems with hidden periodicity (factoring, discrete-logarithm)	Problems with no periodicity (optimization, sampling)

in bits. Then, the optimum solution (state) is identified by some means and the probability amplitude of this state is increased by $2/\sqrt{2^N}$ with a linear interference effect, while the probability amplitudes for all the other states are decreased by a small amount to satisfy the normalization condition. By repeating this process (Grover iteration) $\sqrt{2^N}$ times, the probability amplitude for the solution state reaches one and those for all the other (non-solution) states are reduced to zero, as shown in Fig. 1(a). Then, a simple projective measurement along the computational basis reports the optimum solution.

In order to implement the Grover algorithm for an N-bit problem, $128(N-3)$ two-qubit (C-NOT) gates and $64(N-3)$ one-qubit gates must be cascaded[7]. Suppose an ideal quantum processor with no decoherence, no gate error and all-to-all qubit coupling will operate at a clock frequency of 1 GHz, i.e. both one and two qubit gates can be implemented with 1 nsec time interval no matter how far two qubits are separated, one Grover iteration for an N-bit problem can be implemented with a time of $2 \times 10^{-7} N$ (sec). Therefore, the entire computational time of finding an optimal solution is $T = 2 \times 10^{-7} N\sqrt{2^N}$(sec). The actual computation times for $N = 20$, 50, 100, 150 bit problems are 4×10^{-3}(s), 6×10^{2}(s), 2×10^{10}(s) and 6×10^{17}(s), respectively, as shown in Table II. This result demonstrates how the exponential scaling law, $\sqrt{2^N}$, of the Grover iteration places a serious limitation on the unitary quantum computation for the applications to combinatorial optimization problems. Since the Grover algorithm is optimum for an unstructured data search problem, no further

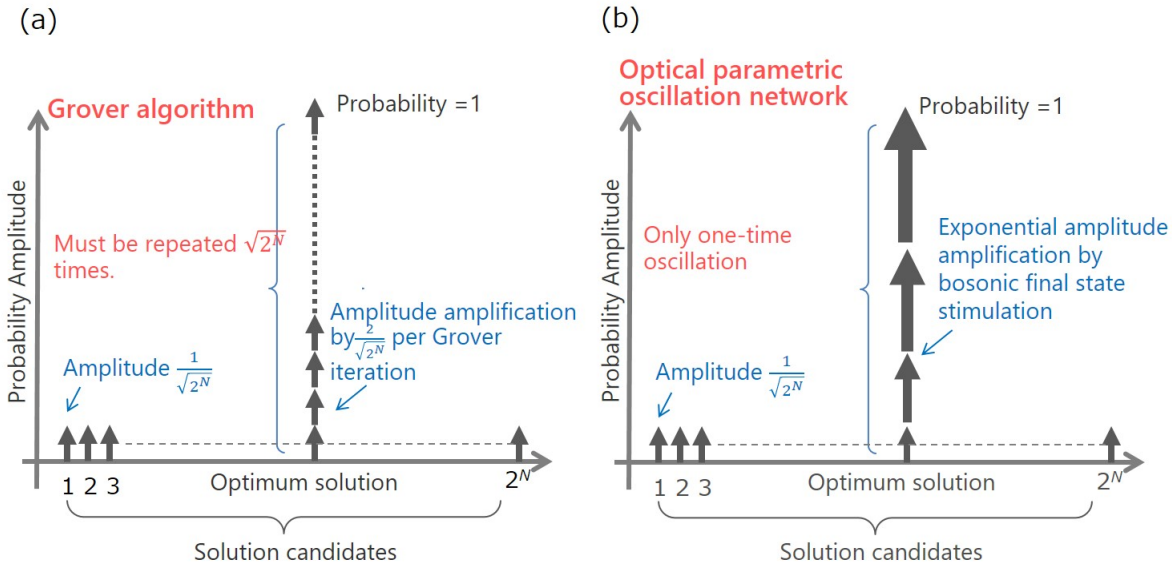

Figure 1: Linear and exponential amplification of the probability amplitude of an optimum solution state in gate-based quantum computer with Grover algorithm and quantum neural network with optical parametric oscillator network.

improvement on the computational time is expected. However, this quantum computation model is universal, i.e. no matter how hard a particuler problem instance is, the Grover iteration promises to return an exact solution with a given computation time, which is a remarkable result already.

More recently, a heuristic quantum algorithm for obtaining an approximate solution rather than an exact solution has been proposed[8], but the problem-size dependent computational time and solution accuracy of this Quantum Approximate Optimization Algorithm (QAOA) are not yet established. Rigetti Computing has implemented the QAOA in thier 19-bit gate-based quantum computer and obtained the computational time of 600 (s) for the $N = 19$ MAX-CUT problem[9].

The adiabatic quantum computation model was proposed to solve an Ising model (or MAX-CUT problem) which is one of the representative combinatorial optimization problems[10, 11]. The D-WAVE Systems manufactured a quantum annealer based on this concept, in which 2000 qubits are sparsely connected by the Chimera graph geometry. This machine can solve an arbitrary MAX-CUT problem with a problem size up to $N = 64$[12]. Table II shows the experimental computation time for $N = 20$ and 50 and also the expected computation time for $N = 100$ and 150 if a larger-size quantum annealer will be available in a future[12]. A specific MAX-CUT problem chosen as a benchmark problem is a random

Table II: Time to solution in the universal quantum computer and three quantum heuristic machines for the MAX-CUT problems with 50% edge density.

Problem Size (number of nodes)	Universal Quantum Computation *	Heuristic Quantum Computation		
		Gate Model Quantum Computer **	Quantum Annealer ***	Quantum Neural Network ****
N = 20	4 x 10^{-3} (s)	600 (s)	1.1 x 10^{-5} (s)	1.0 x 10^{-4} (s)
N = 50	6 x 10^{2} (s)	---	5.0 x 10 (s)	3.7 x 10^{-4} (s)
N = 100	2 x 10^{10} (s) (∼700 years)	---	∼10^{17} (s) ∼3.5B years	2.5 x 10^{-3} (s)
N = 150	6 x 10^{17} (s) (∼20B years)	---	(∼10^{32} (s))	5.4 x 10^{-2} (s)

* Theoretical limit (no decoherence, no gate error, all-to-all connections, 1 nsec gate time)
** Experimental time for 19-bit gate-based quantum computer of Righetti Computing (QAOA has been implemented.)
*** Experimental time for D-WAVE 2000Q (N = 20, 50) and expected time (N = 100, 150)
**** Experimental time for NTT 2000 CIM (N = 20, 50, 100, 150)

graph with an edge density of 50%. This particular machine (D-WAVE 2000Q) has sparse connectivity among qubits, so that only the problem size less than $N = 64$ bits can be embedded into the machine and solved. The computation time to a solution is 1.1×10^{-5} (s) and 5.0×10 (s) for $N = 20$ and 50 and has a problem size dependence of $\exp(cN^2)$ for $N \leq 50$, where c is a constant. This result is related to the fact that $\sim O(N)$ physical qubits must be used to embed the N-bit arbitrary graph using the minor embedding technique. If we extend this trend to $N = 100$ and 150, we have the estimated computation time of $\sim 10^{17}$ (s) and $\sim 10^{32}$ (s), respectively.

Since the beginning of this century, scientists have looked into the possibility of finding a new quantum computational model which fits well to combinatorial optimization problems with no hidden periodicity. One of such efforts is the dissipative quantum computation[5, 6].

The dissipative quantum computation can be realized in an open-dissipative system which couples to external reservoirs and naturally such a machine exists at the quantum-to-classical crossover regime rather than in the genuine quantum substrate[5]. The dissipative coupling to external reservoirs usually destroys the useful quantum effects, but in some cases the dissipation becomes a very powerful computational resource[6]. Quantum chaos in coherent

SAT machines (CSM) and quantum Darwinism in coherent Ising machines (CIM) are such examples. Those two machines are the constituent members of quantum neural network and described in detail in Chpaters VI and VII of this white paper, respectively. The theoretical description for such an open-dissipative quantum machine is complicated and the physical picture is not simple to establish. However, this type of quantum computer is inherently robust against gate errors and external noise injection, because the solution is self-organized in the steady state through the "einselection" by the joint interaction of the system, the reservoirs and the observer (measurement-feedback circuit). The difference in the unitary quantum computation and dissipative quantum computation models are summarized in Table I.

As shown in Fig. 1(b), the probability amplitude for an optimum solution is amplified exponentially in the coherent Ising machines (CIM) due to the spontaneous symmetry breaking followed by the stimulated emission of photons at optical parametric oscillator (OPO) threshold, so that the exponential scaling ($\sim \sqrt{2^N}$) of the computation time in the unitary quantum computation with Grover's algorithm can be overcome. In CIM, the cost function of a combinatorial optimization problem is mapped onto the loss of the degenerate optical parametric oscillator (DOPO) network and an optimum solution with a minimum loss can be obtained as a single oscillation mode[13, 14]. The exponential increase of the probability amplitude of an optimum solution is made possible by the onset of bosonic final state stimulation into a single oscillation mode at above the DOPO threshold.

When a quantum system is dissipatively coupled to external reservoirs, the specific quantum state is chosen in the system through the joint-stabilization process between the system and reservoirs. This self-organization process of the specific quantum state in an open quantum system is called "quantum Darwinism"[5]. A particular machine which is a member of QNN, coherent Ising machine (CIM), can solve NP-hard Ising problems by exploiting the quantum Darwinism as a fundamental operational principle.

When an analog neural network with multiple layers has asymmetric coupling constants between different layers, such a network is often captured by periodic solutions or chaotic traps. This is a serious source of failure in recurrent neural networks for combinatorial optimization. However, it is known that classical chaos is suppressed effectively in quantum systems due to the stretching, folding and destructive interference of the probability amplitudes in a phase space. This suppression mechanism of classical chaos is called "quantum

chaos"[5]. A particular machine which is another member of QNN, coherent SAT machine (CSM), can solve NP-complete k-SAT problems by exploiting the quantum chaos as a fundamental operational principle. The QNN consists of the above CIM and CSM as two main building blocks and implements the dissipative quantum computation model with optics. One of the QNN's unique features is that it is robust against external noise injection and gate errors, since the whole computation process is a self-organization process in such an open dissipative setting.

The classical analog of CIM was proposed as the network of injection-locked lasers, in which a coherent mean-field produced at above the oscillation threshold searches for the ground state of an Ising Hamiltonian and a single lasing mode with a minimum overall loss corresponds to the desired solution[15]. In 2013, the concept was extended to the network of degenerate optical parametric oscillators (DOPO), in which the intrinsic quantum uncertainty of the squeezed vacuum state, formed in each DOPO at below the oscillation threshold, searches for the ground state of Ising problems. Table II summarizes the experimental computation time to the solution by the QNN (CIM) for the MAX-CUT problems with an edge density of 50%[12].

The DOPO network based quantum neural network (QNN) has the following distinct properties in its constituent element, a quantum neuron:

1. Each DOPO is prepared in a superposition state of different in-phase amplitude eigenstates $|X\rangle$ so that a quantum parallel search, involving either quantum entanglement or quantum tunneling, can be realized.

2. A network of DOPOs makes a decision to select a computational result by spotaneous symmetry breaking at a critical point of DOPO phase transition.

3. A network of DOPOs amplifies the selected solution from quantum (microscopic) level to a classical (macroscopic) level via bosonic final state stimulation at above the oscillation threshold.

The other constituent element for QNN is a quantum synapse which connects two quantum neurons with a given coupling constant $[J_{ij}]$. There are two ways of implementing quantum neural networks (QNN); one is based on an optical delay line coupling scheme (DL-QNN) and the other is based on a measurement feedback coupling scheme (MF-QNN). These

two machines use distinct quantum parallel search mechanisms: quantum entanglement formation for DL-QNN and quantum tunneling for MF-QNN. Both schemes can implement not only undirectional neural network but also directional recurrent neural network, which possesses a unique function of error detection and correction. The two schemes have the following differences:

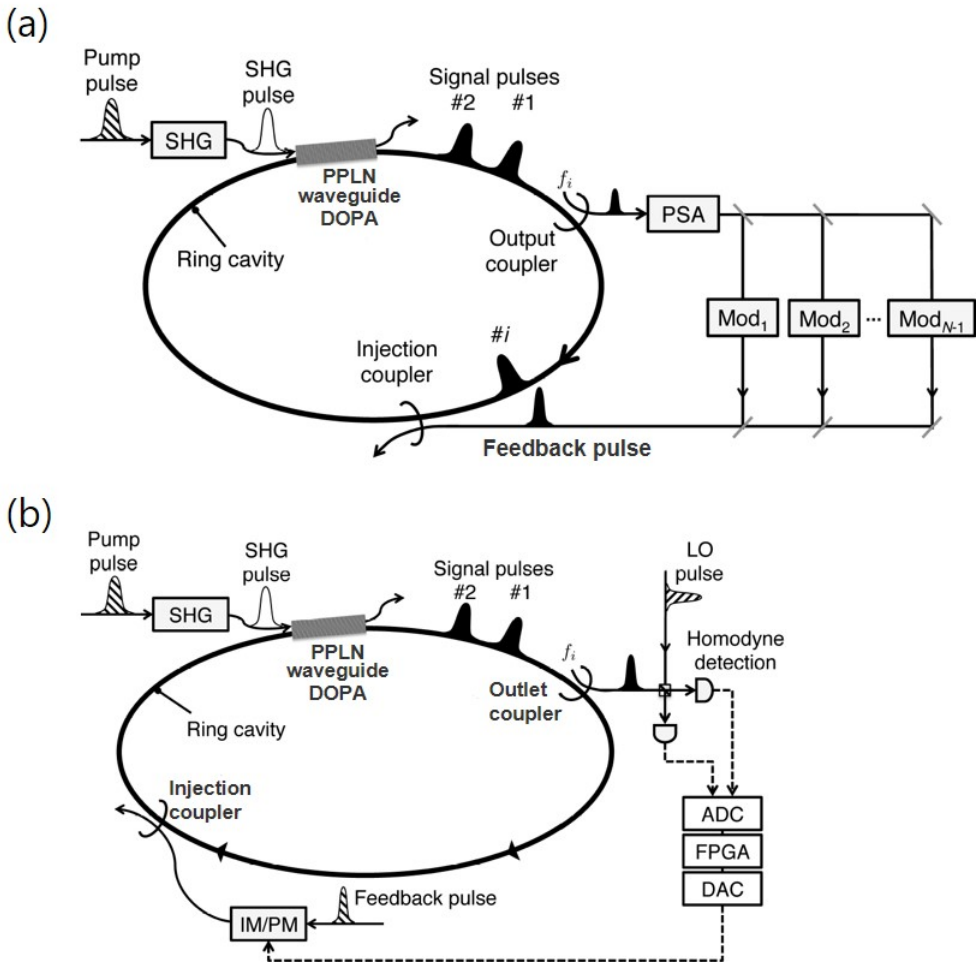

Figure 2: Two types of coherent Ising machines (CIM). (a) A coherent Ising machine (CIM) based on the time-division multiplexed DOPO pulses with mutual coupling implemented by optical delay lines. A part of each pulse is picked off from the main cavity by the output coupler followed by an optical phase-sensitive amplifier (PSA) that amplifies the in-phase amplitude $\hat{X}$ of the extracted DOPO pulse. The feedback pulses, which are produced by combining the outputs from $N-1$ intensity and phase modulators, are injected back to the target DOPO pulse by the injection coupler[16–18]. (b) A CIM with a measurement-feedback circuit. A small portion of each DOPO signal pulse is out-coupled through the output coupler, and its in-phase amplitude is measured by optical balanced homodyne detectors, where LO pulse is directly obtained from the pulsed pump laser. Two detector outputs are converted to digital signals and input into an electronic digital circuit, where a feedback signal for the ith DOPO signal pulse is computed. The feedback pulse also taken from the pump laser is modulated in its intensity and phase to achieve the target amplitude proportional to $\sum_j J_{ij}\bar{X}_j$ and coupled into the ith signal pulse by an injection coupler. Flows of optical fields and electrical signals are shown as solid and dashed lines, respectively[19, 20].

1. In the optical delay line coupling scheme[16–18] shown in Fig. 2(a), a part of the internal DOPO pulse field is extracted and injected back to the target DOPO pulse after an appropriate delay and modulation are introduced based on the Ising coupling matrix $[J_{ij}]$. The DOPO pulses become entangled by such a direct optical coupling and the produced quantum correlation forces the DOPO network selects a ground state of the Ising Hamiltonian when the system breaks a symmetry spontaneously at the oscillation threshold.

2. In the measurement-feedback scheme[19, 20] shown in Fig. 2(b), the internal DOPO pulse amplitude is measured approximately by homodyne detectors, which results in the partial reduction of the wavefunction of the measured DOPO pulse. Furthermore, the feedback signal injection displaces the wavefunction of the target DOPO pulse. The reduction of the measured wavefunction and the displacement of the target wavefunction jointly realize the correlated quantum tunneling, which produces the correlation between the average amplitudes, the centers of gravity of the two wavefunctions, according to the $[J_{ij}]$ matrix. The produced correlation forces the DOPO network selects a ground state of the Ising Hamiltonian when the spontaneous symmetry breaking is kicked in at the oscillation threshold.

The two coupling schemes are compared in Table III.

If a network of DOPOs is arranged into a layered neural network with directional coupling constants $J_{ij} \neq J_{ji}$ between different layers, such a recurrent network can find efficiently the satisfying solutions of NP-complete k-SAT problems. Quantum uncertainty is utilized as a useful computational resource which realizes the destructive interference in a phase space to avoid chaotic traps in this case.

In a slightly wider scope for next-generation computing systems, various alternative approaches to modern von-Neuman type computers have been intensively explored in recent years. There are at lease four approaches actively studied in the current efforts, which are

1. Return to analog computers
2. Learn from nature
3. Mimic human brains
4. Utilize quantum effects

QNN has all of the four aspects mentioned above and it is hard to identify its membership to

Table III: Optical delay line coupling machine (DL-QNN) vs. measurement-feedback coupling machine (MF-QNN)

	DL-QNN [16-18]	MF-QNN [19,20]
Implementation	$(N-1)$ optical delay line with dynamic modulation based on $[J_{ij}]$	Single measurement-feedback loop consisting of homodyne detector, ADC-FPGA-DAC circuit and optical modulator
Quantum parallel search	Quantum correlation (Entanglement, Discord)	Quantum tunneling
Pros	▪ High-speed operation ▪ Both classical and quantum Hamiltonians	▪ Robust against optical loss and phase noise ▪ High-order Ising couplings $(\sigma_1\sigma_2\sigma_3\cdots)$
Cons	Sensitive to optical loss and phase error	Speed limit imposed by electronics
Applications	▪ Quantum simulation ▪ Large-scale problems with regular/sparse connections	▪ Classical Hamiltonian (combinatorial optimization) ▪ Medium-scale problems with irregular/dense connections

a specific category. From the viewpoint of the category 1, the DOPOs can be considered as analog processors and memories which are relatively robust against gate errors and external noise injection. If we take a classical limit in the theoretical model of QNN, we can recover the Hopfield-Tank analog neural network model. This fact allows QNN to solve not only a combinatorial optimization problem but also a continuous-variable optimization problem. From the viewpoint of the category 2, the DOPOs make a decision on the final result by choosing a single oscillation mode in either 0-phase coherent state or π-phase coherent state at a DOPO threshold in a correlated way. After this spontaneous symmetry breaking (or supercritical pitchfork bifurcation) happens, bosonic final state stimulation is kicked in and the self-organized order is established a classical and robust system. The whole computational process is analogous to various phase transition phenomena in nature. For instance, QNN computation is analogous to the ferromagnetic or anti-ferromagnetic ordering at critical temperatures. From the viewpoint of the category 3, the quantum dynamics in QNN resemble to the classical dynamics governed by the majority vote among many copies of identical classical neural networks (CNN). The collapse of the wavefunction made by the single quantum system (QNN) can be simulated by many trajectories in the ensemble of

identical CNNs governed by unique measurement results and randam-different noise sources. From the viewpoint of the category 4, quantum parallel search realized by squeezed vacuum states near the oscillation threshold provides an important step to solve an Ising problem and quantum chaos is a key to solve efficiently a k-SAT problem in QNN. The exponentially increasing success rate to find a ground state in QNN stems from the onset of the stimulated emission of photons at above threshold.

This white paper is organized as follows (Fig. 3). Chapter I introduces the basic concepts, operational principles and expected performance of the DL-QNN and MF-QNN. The physics and nonlinear dynamics of degenerate optical parametric oscillators(DOPO) are presented in Chapter II, in which such topics as DOPO phase transition, quantum tunneling and effective temperatures are introduced. The quantum theory for the DL-QNN is presented in Chapter III, where quantum noise correlation expressed by entanglement and discord are identified as the important computational resource of the machine. Chapter IV briefly reviews the theory of quantum measurements, in particular the approximate measurements, continuous nonlinear measurements and contextuality in quantum measurements are formulated. The quantum theory of the MF-QNN is presented in Chapter V, where quantum tunneling induced by wavepacket reduction and displacement are identified as the important computational mechanism of this machine. Chapter VI describes the principles of the coherent Ising machines (CIM) and various benchmark studies against modern algorithms based on numerical simulation. The performance of CIM for NP-hard Ising problems is compared to the four types of classical neural networks: Hopfield network (discrete variables, deterministic evolution), simulated annealing (discrete variables, stochastic evolution), Hopfield-Tank neural network (continuous variables, deterministic evolution) and Langevin dynamics (continuous variables, stochastic evolution). Chapter VII describes the coherent SAT machines (CSM). The performance of CSM for NP-complete k-SAT problems is compared with the classical approaches.

The readers interested in obtaining the minimum knowledge about the basic concepts and principles of the QNN can read Chapter I to achieve this goal. If he/she is interested in the QNN cloud service starting in November, 2017, Chapter VI provides a good summary for this novel computing machine. Finally, those who wish to understand the basic physics and quantum theory of the two types of QNN at a deeper level may read Chapter II - V as well as the above two chapters.

We will release several additional chapters for presenting coherent SAT machines and actual algorithms for real-world problems: drug discovery, wireless communications, compressed sensing, machine learning and fintech in November, 2018.

The organization of the white paper are listed below:

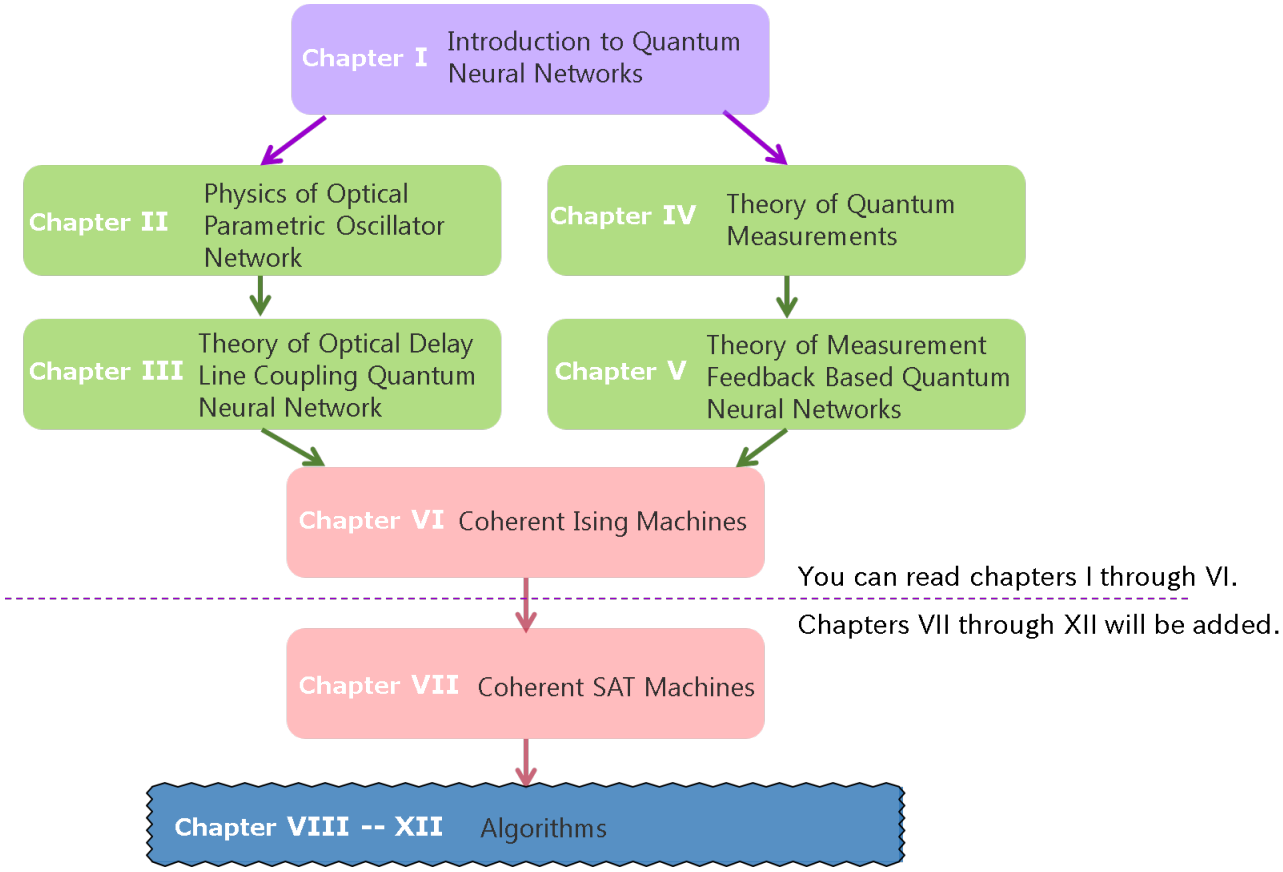

Figure 3: Organization of the white paper.

[1] D. Deutsch, Proc. of the Royal Society of London. Series A, Mathematical and Physical Sciences, 400, 1818 (1985).

[2] P. W. Shor, Proc. of the 35th Annual Symposium on Foundations of Computer Science, IEEE Computer Society Press (1994).

[3] D. Aharonov et al., in Proc. 45th Annual IEEE Symposium on Foundations of Computer Science (FOCS '04), 0272-5428/04 (2004).

[4] L. K. Grover, in Proc. 28th Annual ACM Symposium on the Theory of Computing, p.212 (May 1996).

[5] W. H. Zurek, Rev. Mod. Phys. 75, 715 (2003).

[6] F. et al., Nature Phys. 5, 633 (2009).

[7] M. Nielsen and I. Chuang, Quantum Computation and Quantum Information (Cambridge University Press, Cambridge 2010).

[8] E. Farhi et al., arXiv:1703.06199 (March 2017).

[9] J. S. Otterbach et al., arXiv:1712.05771 (December 2017).

[10] E. Farhi et al., Science 292, 472 (2001).

[11] T. Kadowaki and H. Nishimori, Phys. Rev. E 58, 5355 (1988).

[12] R. Hamerly et al., to be published (2018).

[13] Z. Wang et al., Phys. Rev. A 88, 063853 (2013).

[14] T. Leleu et al., Phys. Rev. E 95, 022118 (2017).

[15] S. Utsunomiya et al., Opt. Express 19, 18091 (2011).

[16] A. Marandi et al., Nature Photonics 8, 937 (2014).

[17] T. Inagaki et al., Nature Photonics 10, 415 (2016).

[18] K. Takata et al., Sci. Rep. 6, 34089 (2016).

[19] T. Inagaki et al., Science 354, 603 (2016).

[20] P. L. McMahon et al., Science 354, 614 (2016).

Written by Y. Yamamoto

version 2